Available online at www.ejournals.uofk.edu

UofKEJ Vol. 7 Issue 1 pp. 8-16 (February 2017)

UNIVERSITY OF KHARTOUM ENGINEERING JOURNAL (UOFKEJ)

Time Series Analysis of H.264 Video

Hiba H. S. M. Ali, Sami M. Sharif

Department of Electronics and Electrical Engineering Department, Faculty of Engineering University of Khartoum, Khartoum, Sudan (E-mail: hiba_im@uofk.edu*)*

Abstract: The aim of this paper is to investigate the statistical properties of H.264/AVC video sequences. The stationarity, dependence properties and self-similarity are investigated. Analysis of the H.264/AVC video sequences variable bit rate (VBR) traffic has shown that this data has strong self-similarity properties as well as noticeable long range dependence (LRD) and short range dependence (SRD). The stationarity of H.264 video sequences is investigated by applying the fractional differencing technique and implemented with Haar maximal overlap discrete wavelet transform. The results indicate that the H.264 video is 2nd order stationary.

Keywords: *Time series analysis; Stationarity; LRD and SRD; H.264 video.*

1. INTRODUCTION

Time series analysis of video traffic is more challenging than for other types of data. This comes as a result of the complex correlation and dependence nature of video data imposed by the encoding technique adopted in video encoding standards, specifically H.26x and Moving Pictures Expert Group MPEG family. These video standards are highly correlated and naturally, they exhibit long memory which is known as long range dependence (LRD).

The analysis process for independent data consists of basic summary statistics; such as mean and variance, and time series analysis checks for trend, seasonality and correlation between data observations. However, for data of strong dependence the time series analysis investigates; basic statistical properties of the data, self-similarity behavior, long range and short range dependence (LRD and SRD) characterization and stationarity property.

This research focuses on video traces of type H.264, also known as MPEG-4 Part 10 Advanced Video Coding Standard (AVC), with its extension of Scalable Video Coding (SVC). This video standard is abbreviated as H.264/AVC with extension SVC. It has significantly improved compression efficiency over its predecessors.

The video data used in this research are scalable, SVC, single layer video traces. There are four H.264 video traces explored in this research. They have the following specifics: Star Wars 4, Silence of the Lambs and Matrix 1 all three are encoded at 30 frames/sec and have GoP G16B7 with the structure IBBBBBBBPBBBBBBB. The fourth video trace; Monsters vs Aliens is encoded at 48 frame/sec and has a GoP of G32B7, IBBBBBBBPBBBBBBBPBBB…. [1]. The 4 video traces times range from 30 minutes to 80 minutes. The techniques presented in this article are applied to all 4 video traces but some results are omitted for brevity. The data has not been edited in any shape or form. This ensures that this analysis represents this type of data accurately.

Time series analysis is adopted in many applications; stock market analysis [2], sales forecasting, process and quality control, medical data analysis [3]. Many researchers have investigated the statistical properties of video data, especially those of Moving Pictures Expert Group (MPEG) video standards, one of these researches is O. Rose report on the statistical properties of earlier versions of MPEG [4]. A more recent study conducted by Pulipaka et al. [5] have investigated the multiplexing characteristics of 3D video formats, in terms of bit rate distortion and bit rate variability.

The most important step of statistical modelling of any time series is to prove that it is stationary, at least in the weak sense of it (section 3.2). This ensures that the statistical properties deduced are reliable and they may be used for designing the statistical model. However, there is a problem in distinguishing between LRD and non-stationary processes since both are characterized by a slow decay of autocorrelation function (ACF). Many researchers have addressed this issue; such as Preuß and Vetter [6]. These researchers developed a FARI (1) bootstrap-based test to discriminate between stationary long range dependence (LRD) and non-stationarity processes.
Researchers in [7] have used discrete wavelet transform to analyze self-similarity and stationarity of long range dependent (LRD) processes. They introduced Log-scale diagram as a means of studying these types of processes. The

wavelet transform was chosen because the coefficients that result from that decomposition, acquire self-similarity and LRD properties naturally. The researchers found that for a self-similar process X(t) which is stationary incremental, the behavior depends on the number of vanishing moments N of the wavelet and the Hurst exponent H. This type of process is also known as H-sssi where H is the self-similar parameter known as Hurst. The relation is: if N > H+1/2, the wavelet coefficients should exhibit short-range correlation only, otherwise, they may exhibit a long-range behavior.

In [8], the authors had applied unit root tests; Dickey-Fuller (DF), Augmented Dickey-Fuller (ADF), Phillips-Perron (PP) and Kwiatkowski-Phillips-Schmidt-Shin (KPSS) to test for stationarity of accumulated Ethernet Traffic. By accumulated; they mean that the data is investigated at different time scales. The authors argued that their results indicate that the accumulated traffic is becoming more stationary as time scale increases.

Another technique that involves testing for homogeneity of variance was introduced by Whitcheret et al. [9]. These researchers developed a test whose null hypothesis is designed to be white noise. They applied discrete wavelet transform (DWT) to LRD time series and argued that the null hypothesis applied to these transformed coefficients have similar rejection rates to the null hypothesis of white noise. They evaluated a normalized cumulative sum of squares test statistic using critical levels for the null hypothesis of white noise.

Till the time of writing this article, no research had been conducted that fully investigates the H.264 video statistical properties. This current research adopts Whitcher's technique for testing of stationarity of H.64 video traces and the data is transformed using Haar wavelet transform and Percival pyramid application of Wavelet transform [10].

2. OVERVIEW OF VIDEO ENCODING

The encoded video has 3 frame types as identified by the Moving Pictures Experts Group (MPEG). They are [11]:

- I-frame: intra-coded.
- P-frame: forward predictive coded with motion compensated prediction from a prior I or P frame.
- B-frame: bi-directional predictive coded. It is encoded using two methods:

a. Classical B frame prediction: in which this frame type is encoded with motion compensated prediction from the prior as well as later I or P frames. It is the default technique of H.264/AVC.
b. Generalized B frame concept: in which this frame type may be encoded with motion compensated prediction from another B frame[12]. That concept was the basis for hierarchical B frame prediction, which is the default for H.264/ SVC (Scalable Video Coding).

I.Hierarchical B frame Encoding

The hierarchy of the B frames in H.264 SVC usually follows a dyadic pattern. Hence, the number of B frames between successive I and P frames is given by,

$$\beta = 2^{\tau} - 1 \quad (1)$$

Where τ = the number of enhancement layers.
Hence, the number of enhancement layers is calculated by,

$$\tau = log_2(\beta + 1) \quad (2)$$

II.Scalable Video Encoding

The video is hierarchically encoded into a base layer and enhancement layer/s. This encoding delivers higher compression rate than its predecessor, H.264/ AVC. It, also, offers several video qualities.

There are several types of scalability supported in H.264/ SVC. They are [12]:

- Temporal scalability: frame frequency is based on hierarchical B frame structure. Dropping each higher order enhancement layer halves the frame frequency. For example, if we have 1 base layer and 2 enhancement layers and a full frame frequency of 30 frame/s, dropping enhancement layer 2 reduces the frame frequency to 15 frames/sec.
- Spatial scalability: different spatial frame resolution. For example, the format for base layer could be CIF 352x288 pixel while the format for base & enhancement layer is 4CIF 704 x 576.

Quality (SNR) scalability: the SNR of video frames varies from one layer to the other. Example, H.264 SVC Coarse Grain Scalability (CGS): It provides up to 8 quality layers with increasing SNR [12].

3. TIME-SERIES ANALYSIS

Analyzing the dependence and correlation amongst individual frames is crucial for appropriate distribution fitting.

3.1. Testing for Stationarity

The time-series could be independent, short range dependent or long range dependent. Thus the time-series should be tested for dependence first. For the dependent and SRD time-series, the most commonly employed techniques to test for stationarity of time-series data are[13], [8]:

- Graphical representation: Sequence plots. They can indicate whether the mean and variances are constant or not.
- Auto-correlation functions: The ACF plot may be an indicator for stationarity if all of the values are contained within a specific range, called confidence range. However, there are many instances where this

condition could not be imposed, for example; the existence of LRD.

- Statistical tests: Augmented Dickey–Fuller (ADF) test, Phillips–Perron (PP) test and Kwiatkowski–Phillips–Schmidt–Shin (KPSS) tests.

Both ADF and PP tests are unit root tests. They test the null hypothesis that a time series has a unit root, which is against the stationarity requirement of all zeros should lie outside the unit circle. The KPSS test is used to test a null hypothesis that the time series is trend stationary.

3.2. Types of Stationarity

A time-series stochastic process {Xt} is considered stationary if the basic statistical properties of mean, variance and covariance do not change over time and neither does the shape of its distribution.

There are two main types of stationarity; strictly stationary and weakly (second-order) stationary [14].Definition 1: A stochastic process {Xt} where t ε I and for any n > 0, t1, t2, ….., t n is a sequence of increasing time indices is strictly stationarity if it satisfies the following requirements;

- The mean and variance remain constant over time.
- The joint distribution$X_{t_1}, X_{t_2}, \ldots\ldots, X_{t_n}$ is the same as the joint distribution for all t1, t2… tnand for all choices of s, such that (tk + s) ε I ∀ k .

A process {Zt} is weakly (second order) stationary, if it has the following properties:

- Mean and variance remain constant over time.
- The covariance; Cov(Zt, Zt-k) = Cov(Z0 ,Zk) for all time t and lag k, where k ≥ 0.

Most real data are second order stationary, also known as wide sense stationary.

3.3. Stationarity of LRD Processes

The LRD processes have a long memory; this will often lead to erroneous rejection of the null hypothesis of the mentioned ADF, PP and KPSS tests. Hence, results obtained from those tests are not final, further investigation needs to be implemented.

Data that exhibits LRD and hence self-similarity is best analyzed using the fractional differencing technique. Hence, this research implements the technique proposed by Whitcher et al [9]. It is based on applying the discrete wavelet transform to the time series data and then testing a hypothesis that states that variances at various scales are equivalent.

Definition 2: if $X_0, \ldots, X_{N-1}$ is a time series that may be regarded as a sequence of independent Gaussian random variables with zero means and variances $\sigma_0^2, \ldots, \sigma^2_{N-1}$ and N is the number of scales of the decomposed series [9]. The hypothesis to be tested is

$$H_0: \sigma_0^2 = \sigma_1^2 = \cdots = \sigma_{N-1}^2 \quad (3)$$

Then the accumulation of variance in time series is computed via the normalized partial energy sequence of X_t, the statistic P_k given by

$$P_k = \frac{\sum_{j=0}^{k} X_j^2}{\sum_{j=0}^{N-1} X_j^2}, k = 1, \ldots, N-1 \quad (4)$$

If the time series satisfies H_0, then P_k is expected to follow a 45° line closely. The deviation from the 45° line is measured against critical values obtained from standard statistical theory. However, for our purposes, the comparison with the 45° line gave satisfactory results without the need for further investigation.

The parameter P_k is calculated for both the detail and approximation coefficients, from j=1,….,k, of the wavelet transformed data.

3.4. Self-Similarity

A time series is considered self-similar if it looks the same when viewed on different time scales, which indicates that the data has the same statistical properties on different time scales.
The degree of self-similarity is measured using Hurst parameter, also known as H exponent. Hurst exponent ranges between 0 and 1, with 0.5<H<1 indicates self-similarity and hence, long range dependence. There are many techniques developed to measure the Hurst parameter, they will not be covered here. For further details, please refer to [15].

Definition 3:A stochastic process X = $\{X(t)\}_{t \square R}$is self-similar if

$$X(at) = a^H X(t), a > 0 \quad (5)$$

Where:

Equality sign ≡ equality in distribution,
a≡ scaling factor,
H≡ Hurst exponent and 1/2<H<1

There are two kinds of self-similar processes, exactly second-order self-similar and asymptotic second-order self-similar.

Definition 4:

1- A process is exactly self-similar with self-similarity parameter H= 1- β/2 and β>0, if, for all m=1,2,…., it has the following properties:

- Variance: Var[X] = $m^{-\beta}$Var[$X^{(m)}$]
- Autocorrelation: R(k, $X^{(m)}$) = R(k, X), k≥ 0 for all m=1,2,…..

2- A process is asymptotically self-similar with parameter H=1- β/2 and β>0, if for m→∝, it has the following properties:

- Variance: Var[X] = $m^{-\beta}$Var[$X^{(m)}$]

- Autocorrelation: R(k, $X^{(m)}$) → R(k, X)

3.5. LRD and SRD of Video Data

A time-dependent process implies common statistical behavior across several time scales. Whether the process is long range or short range depends on the result of investigating its autocorrelation behavior.

Long range dependence: autocorrelations decay hyperbolically.

$$\rho_k(k) \to k^{2H-2} \tag{6}$$

$$\sum_k \rho_x(k) = \infty \tag{7}$$

Short range dependence: autocorrelations decay exponentially.

$$\rho_x(k)\gamma^{-k} \tag{8}$$

$$\sum_k \rho_x(k) \neq \infty \tag{9}$$

4. WAVELET ANALYSIS

The wavelet decomposition has a high impact on the correlation and dependence of data. The multi-scale decomposition removes the serial correlation of a long memory process [9].

The exact behavior depends crucially on the number N of vanishing moments of the wavelet and the Hurst exponent H: if N > H+1/2, the detail coefficients should exhibit short-range correlation only, otherwise, they exhibit a long-range behavior [7].

4.1. Haar Wavelet Analysis

This wavelet basis is a square wave with compact support. It is symmetric but not continuous. Its scaling and wavelet functions are respectively given by equations (10) and (11).

$$\emptyset(t) = \begin{cases} 1 & 0 \le t < 1 \\ 0 & otherwise \end{cases} \tag{10}$$

$$\varphi(t) = \begin{cases} 1 & 0 \le t < 1/2 \\ -1 & \frac{1}{2} \le t < 1 \\ 0 & otherwise \end{cases} \tag{11}$$

4.2. Haar Wavelet and Multi-resolution Analysis

The wavelet function is localized in space, causing wavelet transformed signals to be sparse. This property is the main reason behind its extensive use in the area of video compression and data traffic modelling in general.

Wavelet analysis consists of two major components;

- The wavelet, also known as the mother wavelet $\varphi(t)$, and
- The scaling function $\emptyset(t)$.

The scaling function $\emptyset(t)$is constructed from the mother wavelet $\varphi(t)$[16]. The scaling function compresses/dilates the mother wavelet by a scale of 2 multiple times, while translating it by k steps. Hence, new scaling and wavelet functions are constructed as follows [16].

$$\emptyset_{jk}(t) = 2^{j/2}\emptyset(2^j t - k) \tag{12}$$

$$\varphi_{jk}(t) = 2^{j/2}\varphi(2^j t - k) \tag{13}$$

The scaling function, equation (12) is equivalent to a low-pass filter and it gives approximation coefficients V_j, while the wavelet function, equation (13) is equivalent to high-pass filter and it produces detail coefficients W_j. These coefficients are defined as [12],

$$V_j = Span\{\emptyset_{jk}(t)\} \tag{14}$$

$$W_j = Span\{\varphi_{jk}(t)\} \tag{14}$$

The coefficient j refers to the scale level, or resolution level, of the signal.

A wavelet filter Bank is constructed by applying the pyramid technique, introduced by Don Percival [10]. Percival designed two pyramid approaches that are based on two wavelet transforms; Discrete Wavelet Transform (DWT), and Maximum Overlap DWT (MODWT).

This research adopts the MODWT, more details about this wavelet multi-resolution analysis is explored in [17].

5. RESULTS AND DISCUSSION

As mentioned before, the statistical analysis techniques are applied to four H.264 video traces. They are: Star Wars 4, Silence of the Lambs and Matrix 1 with GoP G16B7 and Monsters vs Aliens with GoP of G32B7. However, some results are omitted for briefness.

5.1. Time Plots of Video Traces

Basic time-series properties are investigated using time plots of the data sequence. These time plots show how data varies with time. The time plots of the whole video, I-Frames, B-Frames and P-Frames of Star Wars are shown in **Fig. 1**. [(a), (b), (c) and (d)] respectively.

The same plots are investigated for Silence of the Lambs as shown in **Fig. 2**. [(a), (b), (c) and (d)], respectively, and the same previous results are obtained.

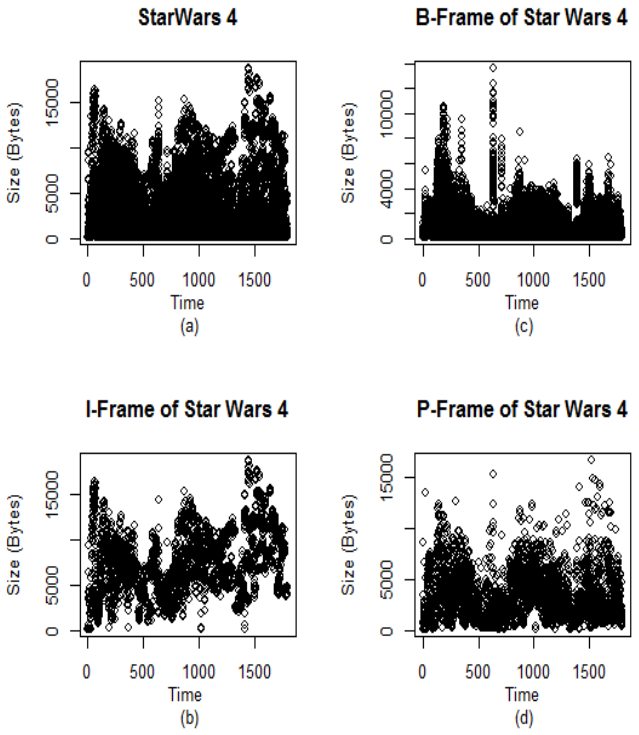

Fig.1. Time Plots of Star Wars 4

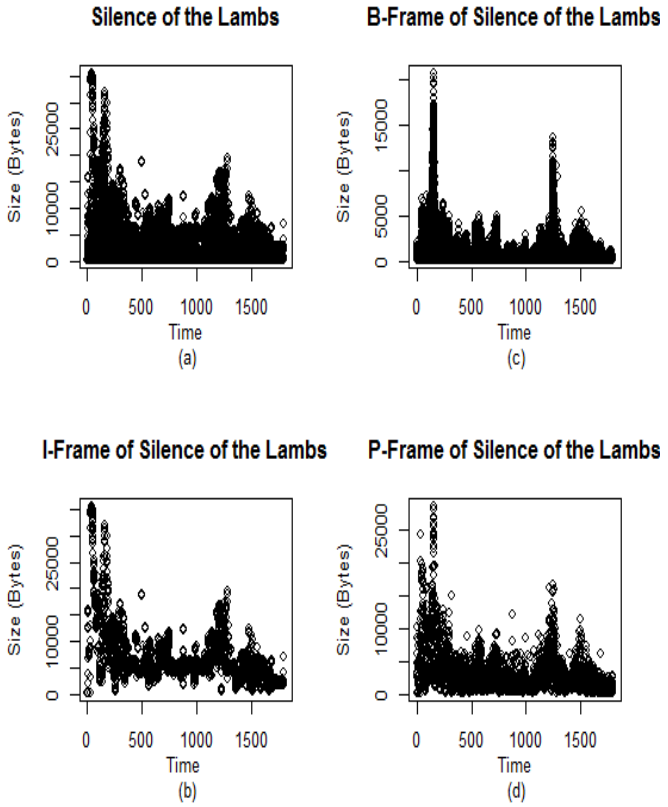

Fig. 2. Time Plots of Silence of the Lambs

In both **Figs 1** and **2** I and P frames follow the same pattern as the original data pattern, while the B-frame has different patterns. This is expected, since the GoP of both Star Wars 4 and Silence of the Lambs is G16B7, i.e. one P-frame in every GoP. There is only one I-frame for every GoP and it follows the same pattern as the whole video, and the P-frame encoding is based on prior I-frame, hence it will follow the pattern of the I-frame. As for the mean and variance, it is not clear from the plots whether they are constant or not.

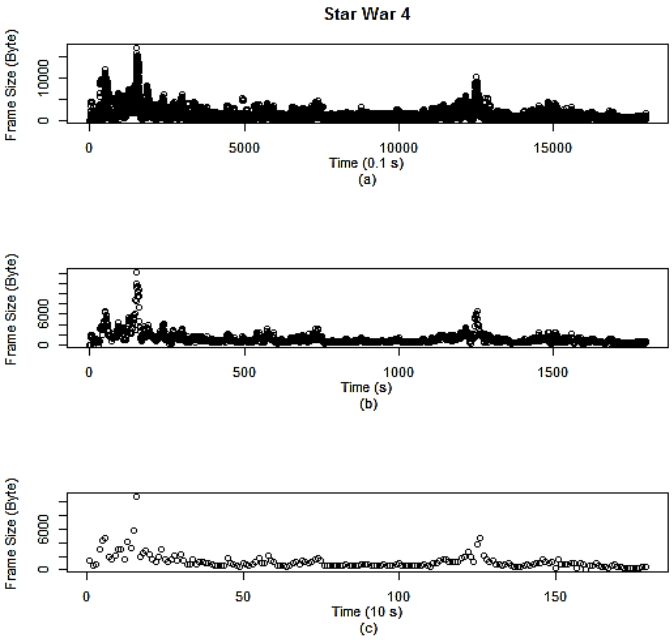

Fig. 3. Aggregated Video Traffic for Star Wars 4

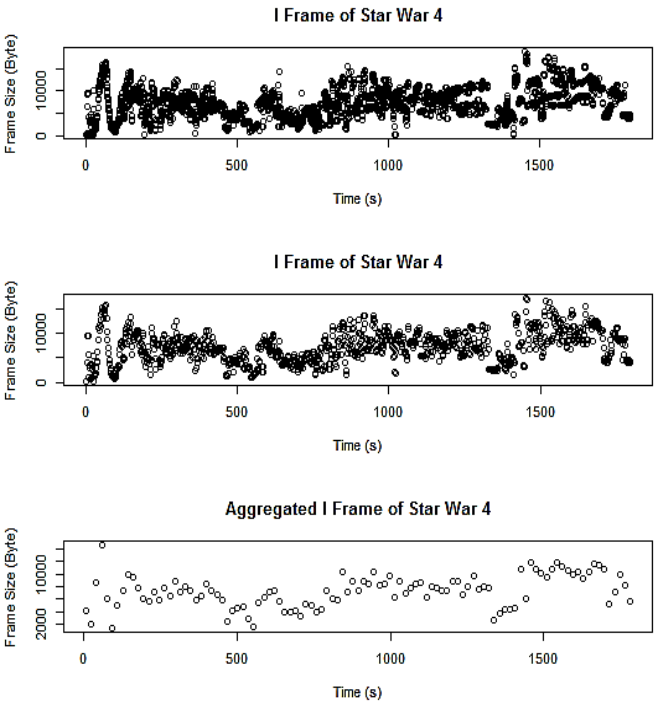

Fig. 4. Aggregated Video Traffic for I-Frame of Star Wars 4

5.2. Self-Similarity of Video Traces

The self-similarity property of video traces is investigated. The results obtained for Star Wars 4 trace file are presented. The aggregated data of the whole video trace and for its I-frame are shown in **Figs 3** and **4**, respectively. They clearly indicate that the video traffic exhibits self-similarity. Those same results apply for the B & P frames as well. The existence of self-similarity indicates that the data has the same statistical properties on different time scales.

5.3. Hurst Parameter

The Hurst parameter is computed using R/S Hurst estimator. The results are shown in Table 1. All tested video traces have Hurst values of more than 0.8 which indicates strong self-similarity of these video traces.

5.4. Investigating LRD and SRD of H.264 Video Traces

The autocorrelation function (ACF) plots are shown in **Fig 5-8** for *Star Wars 4* and *Silence of the lambs* video traces respectively. As explained in section 4(G), the ACF is monitored for the way it decays. The way it subsides to zero value or more accurately to a chosen confidence level around zero is investigated. This research uses 95% confidence level. This confidence range is indicated in these plots by the two dashed blue line. The short range dependence is tested by investigating 50 time lags, while the long range dependence is investigated by 300 time lags.

The 4 plots show that I-frames may exhibit LRD and SRD as well as the P-frames, but the B frames have LRD only on both video traces, this could be a direct outcome of the encoding procedure of B-frames, since they are encoded with respect to past and previous values of I, P and sometimes even B frames.

This indicates that variable bit rate, VBR, video exhibits both LRD and SRD. Hence a model that can capture both dependencies is needed.

Table 1. Hurst Parameter using R/S estimator

Video Trace	Hurst exponent
Star Wars 4	0.8629008
Monsters vs Aliens	0.9192828
Silence of the Lambs	0.9487634
Matrix 1	0.8582841

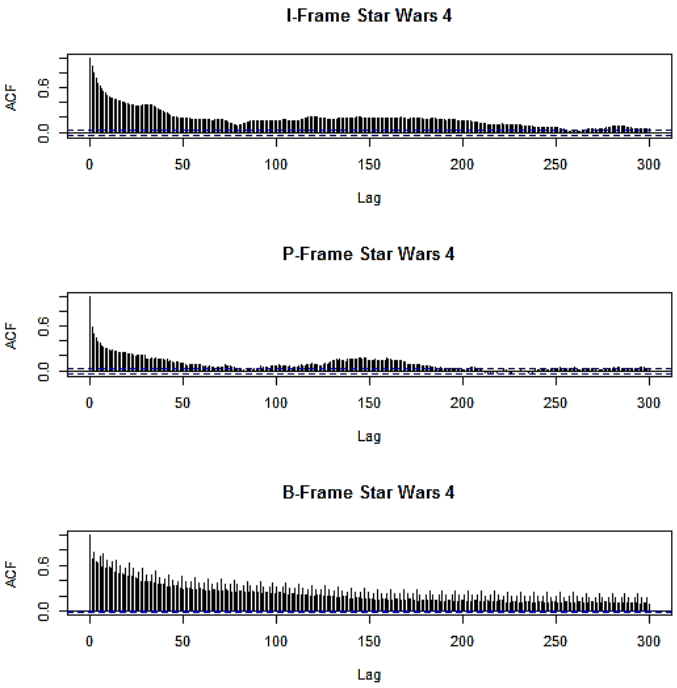

Fig. 5. ACF of I, P and B Frames sizes for Star Wars 4, LRD

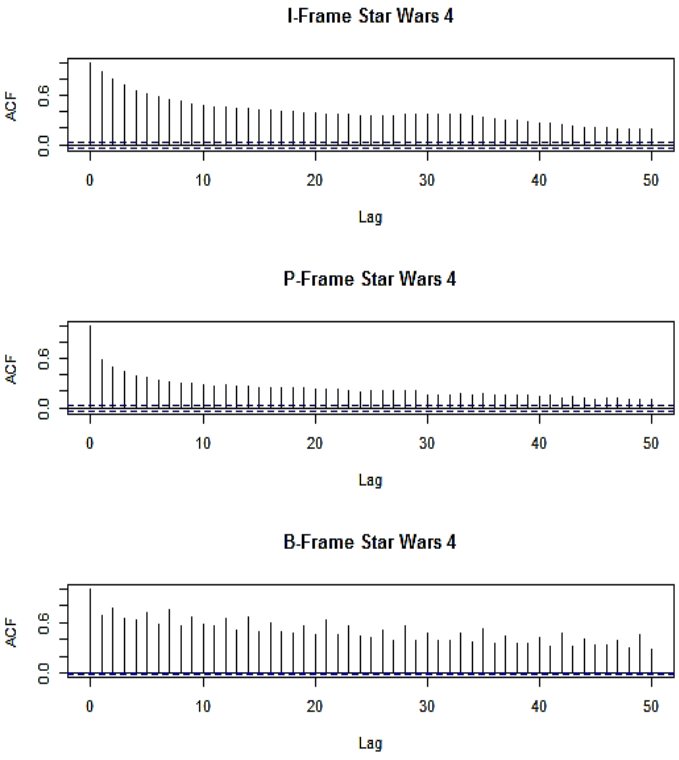

Fig. .6.ACF plots of I, P and B Frames of Star Wars 4, SRD

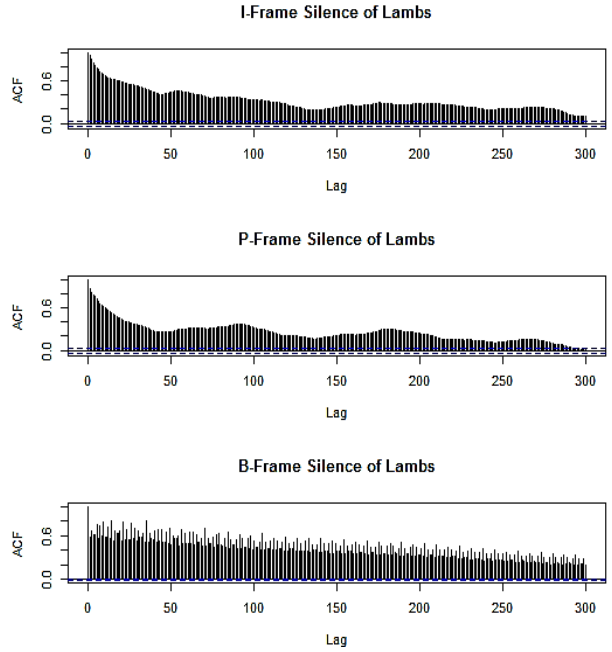

Fig. 7. ACF of I, P and B Frames of Silence of the Lambs, LRD

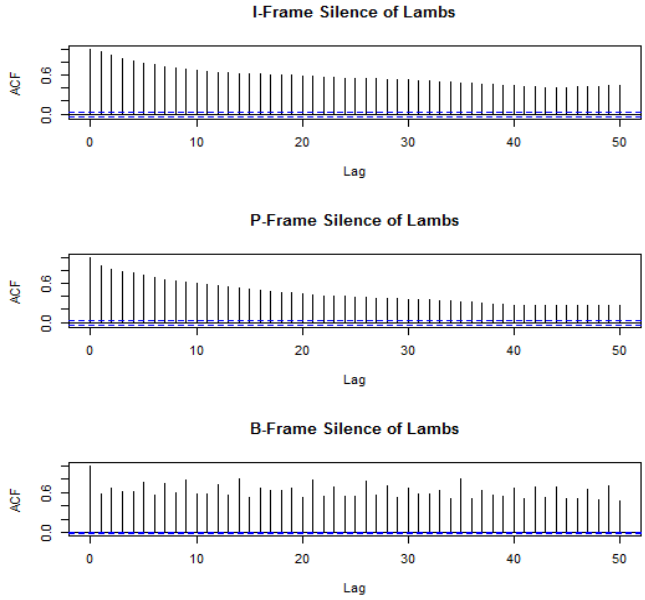

Fig. 8. ACF of I, P and B Frames of Silence of the Lambs, SRD

5.5. Stationarity of Video Data

As shown by the results of **Figs 3-8,** the H.264 video traces exhibit SRD, LRD and self-similarity. Thus, it is a perfect candidate for applying fractional differencing, as mentioned before.

The Whitcher technique described earlier is applied, and the parameter Pk calculated for both the detail and approximation coefficients are plotted vs the octave (scale) number. For homogeneous variance, this plot should follow a 45° line closely.

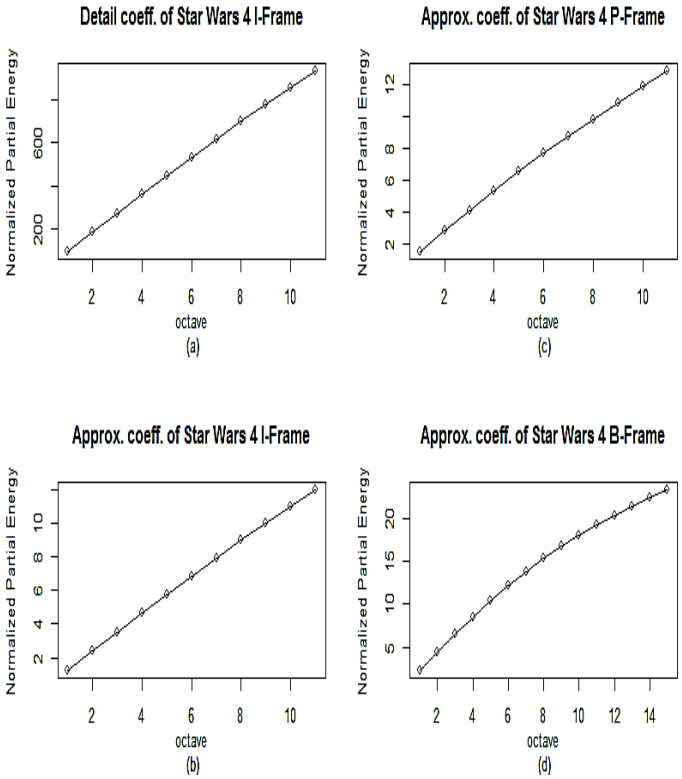

Fig. 9. Wavelet Variance for Star Wars 4: (a) I-Frame Detail Coefficient, (b) I-Frame Approximation Coefficients, (c) P-Frame Approximation Coefficients, (d) B-Frame Approx. Coefficients

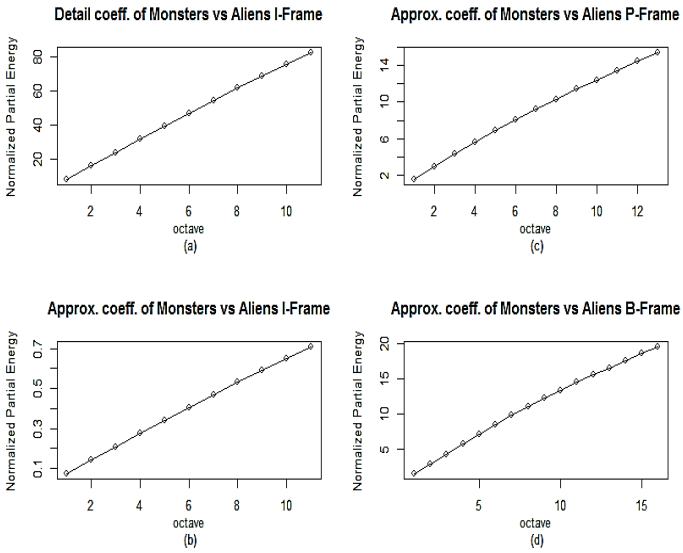

Fig. 10. Wavelet Variance for Monsters vs Aliens: (a) I-Frame Detail Coefficient, (b) I-Frame Approximation Coefficients, (c) P-Frame Approximation Coefficients, (d) B-Frame Approx. Coefficients

The results obtained in Figure (9), (10) and (11) show that the parameter P_k follows a 45 line closely, as an indicator that variances at different scales are equivalent and hence the series shows 2nd order stationarity.

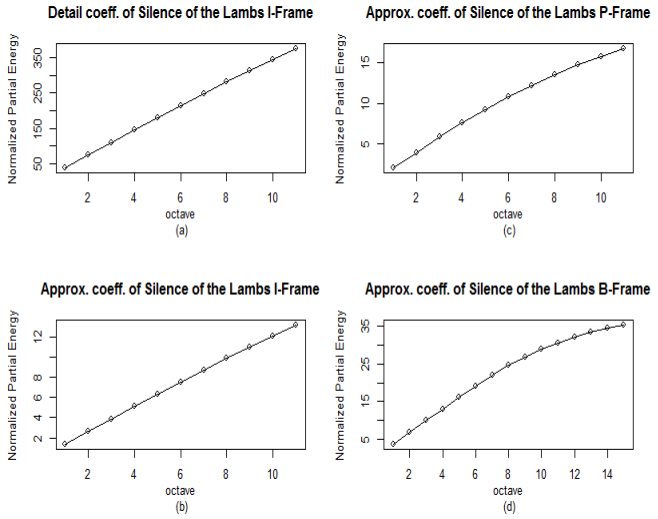

Fig. 11. Wavelet Variance for Silence of the Lambs: (a) I-Frame Detail Coefficient, (b) I-Frame Approximation Coefficients, (c) P-Frame Approximation Coefficients, (d) B-Frame Approx. Coefficients

As a further measure the ADF and KPSS are calculated as well and their results are shown in **Table 2** for some coefficients of wavelet decomposed I-Frame of Star Wars 4 and **Table 3**, for Monsters vs Aliens. The data column indicates the coefficient type and level by Wj and Vj for detail and approximation coefficients respectively. The two statistical tests p values are shown in the second and third column.

The ADF and KPSS test results for Star Wars 4 and Monsters vs Aliens are shown in Table 2 and 3 respectively.

Table 2.ADF and KPSS Results for Star Wars 4

Data	adf.test	kpss.test
iwt.W.W2	0.01	0.10
iwt.W.W3	0.01	0.10
iwt.W.W6	0.01	0.10
iwt.V.V2	0.01	0.01
iwt.V.V3	0.01	0.01
iwt.V.V6	0.01	0.01

Table 3.ADF and KPSS Results for Monsters vs Aliens

Data	adf.test	kpss.test
iwt.W.W2	0.01000000	0.10000000
iwt.W.W3	0.01000000	0.10000000
iwt.W.W6	0.01000000	0.10000000
iwt.V.V2	0.01000000	0.01100768
iwt.V.V3	0.01000000	0.01000000
iwt.V.V6	0.03120218	0.01000000

As mentioned before, the ADF and KPSS results are not conclusive for time series with long range dependence. Tables 2 and 3 indicate that the detail coefficients are stationary since the ADF test result is 0.01 and the KPSS test for trend stationarity is 0.1, signifying that the hypothesis is fulfilled. However, the test results for both video traces; Star Wars 4 and Monsters vs Aliens, gives contradictory results for the approximation coefficients, since the two tests gives low p values, hence no stationarity could be concluded.

This is expected since the approximation coefficients are low pass filtered from the original time series, hence they follow the same dependence structure of the original data, while the detail coefficients are high pass filtered. This latter process reduces the temporal correlation in the input time sequence. This transforms signals with LRD properties to produce short-range dependent wavelet coefficients and thus introduces 2nd order stationarity.

6. CONCLUSIONS

In this paper the statistical parameters of the H.246/AVC video sequences were investigated by applying the fractional differencing technique and implemented using Haar maximal overlap discrete wavelet transform on the I, P and B frames of the data sequences. The results indicate that the H.264 video is 2nd order stationary. Four video sequences with different GoP were considered here: Star Wars 4, Silence of the Lambs, Matrix 1 and Monsters vs Aliens. The analysis of these video sequences has shown that both the I and P frames follow the same pattern as the original data pattern, while the B-frame has different patterns. The self-similarity property of video traces is investigated by calculation of the Hurst Parameter using R/S estimator. Results showed that, all tested video traces have Hurst values of more than 0.8 which indicates strong self-similarity of these video traces. Furthermore, the dependency test showed that the variable bit rate, VBR, video exhibits both LRD and SRD.

Acknowledgement

The authors are grateful to Engineer Fabric Clerot, Orange Labs, Moylan, France whose online discussions were invaluable to this research.

REFERENCES

[1] P. Seeling and M. Reisslein, "Video transport evaluation with H.264 video traces," IEEE Commun. Surv. Tutorials, vol. 14, no. 4, pp. 1142–1165, 2012.

[2] M. Qiu and Y. Song, "Predicting the direction of stock market index movement using an optimized artificial neural network model," PLoS One, vol. 11, no. 5, May 2016.

[3] L. Hussain et al., "Symbolic time series analysis of electroencephalographic (EEG) epileptic seizure and

brain dynamics with eye-open and eye-closed subjects during resting states," J. Physiol. Anthropol., vol. 36, no. 1, May 2017.

[4] O. Rose, "Statistical properties of MPEG video traffic and their impact on traffic modelling in ATM systems," in Proceedings of the 20th Annual IEEE Conference on Local Computer Networks, 1995, pp. 397–406.

[5] A. Pulipaka, P. Seeling, M. Reisslein, and L. J. Karam, "Traffic and statistical multiplexing characterization of 3-D Video Representation Formats," IEEE Trans. Broadcast., vol. 59, no. 2, pp. 382–389, 2013.

[6] P. Preuß and M. Vetter, "Discriminating between long-range dependence and non-stationarity," Electron. J. Stat., vol. 7, no. 1, pp. 2241–2297, 2013.

[7] P. Abry, P. Flandrin, M. S. Taqqu, and D. Veitch, "Self-similarity and long-range dependence through the wavelet lens," Theory Appl. long range Depend., vol. 59, pp. 527–556, 2003.

[8] Z. Lu, M. Li, and W. Zhao, "Stationarity testing of accumulated ethernet traffic," Math. Probl. Eng., vol. 2013, no. 1, 2013.

[9] B. Whitcher, S. D. Byers, P. Guttorp, and D. B. Percival, "Testing for homogeneity of variance in time series: long memory, wavelet, and the Nile river," Water Resour. Res., vol. 38, no. 5, p. 10.1029/2001WR000509, 2002.

[10] D. Percival, "An Introduction to the Wavelet Analysis of Time Series," Symp. Tutorials, June, vol. 6, p. 2000, 2000.

[11] A. Pulipaka, P. Seeling, and M. Reisslein, "Traffic models for H.264 video using hierarchical prediction structures," in Global Communications Conference (GLOBECOM), 2012 IEEE, 2012, pp. 2107–2112.

[12] P. Seeling, M. Reisslein, and B. Kulapala, "Network Performance Evaluation using Frame Size and Quality Traces of Single-layer and Two-layer Video: A Tutorial," IEEE Commun. Surv. Tutorials, vol. 6, no. 3, pp. 58–78, 2004.

[13] C. Chatfield, The Analysis of Time Series An Introduction, 5th ed. John Wiley & Sons, Inc., 1996.

[14] K. Park and W. Willinger, Self-Similar Network Traffic and Performance Evaluation. New York, USA: John Wiley & Sons, Inc., 2000.

[15] Z. Sahinoglu and S. Tekinay, "On multimedia networks: self-similar traffic and network performance," IEEE Commun. Mag., vol. 37, no. 1, pp. 48–52, 1999.

[16] C.-L. Liu, "A Tutorial of the Wavelet Transform," Natl. Taiwan Univ. Dep. Electr. Eng., pp. 1–72, 2010.

[17] H. H. S. M. Ali and S. M. Sharif, "Computation Reduction of Haar Wavelet Coefficients," in 2017 2nd International Conference on Image, Vision and Computing (ICIVC), 2017, pp. 832–835.